

Intravenous morphine self-administration alters accumbal microRNA profiles in the mouse brain

Juhwan Kim^{1,2}, Heh-In Im^{2,3,4,*}, Changjong Moon^{1,*}

1 Department of Veterinary Anatomy and Animal Behavior, College of Veterinary Medicine and BK21 Plus Project Team, Chonnam National University, Gwangju, South Korea

2 Center for Neuroscience, Korea Institute of Science and Technology (KIST), Seoul, South Korea

3 Convergence Research Center for Diagnosis, Treatment and Care System of Dementia, Korea Institute of Science and Technology (KIST), Seoul, South Korea

4 Division of Biomedical Science & Technology, KIST School, Korea University of Science and Technology, Seoul, South Korea

Funding: This research was funded by the National Research Council of Science & Technology (NST) grant by the Korean government (MSIP) (No. CRC-15-04-KIST) and the National Research Foundation of Korea under the grant (No. NRF-2017R1A2B200399; Mid-career Researcher Program).

Abstract

A significant amount of evidence indicates that microRNAs (miRNAs) play an important role in drug addiction. The nucleus accumbens (NAc) is a critical part of the brain's reward circuit and is involved in a variety of psychiatric disorders, including depression, anxiety, and drug addiction. However, few studies have examined the expression of miRNAs and their functional roles in the NAc under conditions of morphine addiction. In this study, mice were intravenously infused with morphine (0.01, 0.03, 0.3, 1 and 3 mg/kg/infusion) and showed inverted U-shaped response. After morphine self-administration, NAc was used to analyze the functional networks of altered miRNAs and their putative target mRNAs in the NAc following intravenous self-administration of morphine. We utilized several bioinformatics tools, including Kyoto Encyclopedia of Genes and Genomes (KEGG) pathway mapping and CyTargetLinker. We found that 62 miRNAs were altered and exhibited differential expression patterns. The putative targets were related to diverse regulatory functions, such as neurogenesis, neurodegeneration, and synaptic plasticity, as well as the pharmacological effects of morphine (receptor internalization/endocytosis). The present findings provide novel insights into the regulatory mechanisms of accumbal molecules under conditions of morphine addiction and identify several novel biomarkers associated with morphine addiction.

Key Words: nerve regeneration; nucleus accumbens; microRNA; morphine; self-administration; bioinformatics; neural regeneration

Introduction

MicroRNAs (miRNAs) are short (~22 nucleotides) non-coding RNAs that play important roles in the regulation of almost all biological processes, including cell development, proliferation, and differentiation, as well as various neurological functions (Im and Kenny, 2012). miRNAs target their complementary binding sites at 3'-untranslated regions (3'-UTR) of mRNA by binding to argonaute (AGO) proteins in miRNA-induced silencing complexes (miRISCs). Subsequently, miRISCs interact with cytoplasmic deadenylase complexes (e.g., PAN2-PAN3 and CCR4-NOT) that catalyze the deadenylation of mRNA target sites. Additionally, miRISCs repress the translation of mRNA target proteins via inhibition of the eukaryotic initiation factor 4F (eIF4F) complex (Jonas and Izaurralde, 2015). Previous studies have shown that miRNAs play an important role in the effects of addictive drugs, such as cocaine and methamphetamine (Hollander et al., 2010; Im et al., 2010), but few studies have investigated the regulation of miRNAs in morphine addiction.

Although morphine is considered to be the gold standard treatment for moderate-to-severe pain in patients with and without cancer (Dalal et al., 2012; Raphael et al., 2013), its clinical use is limited due to the rewarding effects and high risk of developing tolerance associated with this drug (Fit-

ting et al., 2016). The primary pharmacological action of morphine is mediated by the activation of mu-opioid receptors (MOR), which are distributed throughout mesolimbic regions, such as the ventral tegmental area (VTA), striatum (STR), amygdala (Amy), and medial prefrontal cortex (mPFC) (Parker et al., 2014; Fields and Margolis, 2015; Kim et al., 2016). Furthermore, molecular and cellular changes in the STR are thought to be one of the most important characteristics involved in understanding the phenotypes of various psychiatric disorders, especially addiction (Nestler, 2004; Tan, 2008; Russo et al., 2010; Imperio et al., 2016).

The striatal complex is subdivided into the dorsal striatum (dST) and the nucleus accumbens (NAc), which comprises a reward circuit with the VTA (Beier et al., 2015). It is widely accepted that the VTA-NAc circuit plays diverse roles in the processes underlying mood disorders and psychostimulant-induced rewarding effects (Nestler, 2004; Russo and Nestler, 2013). Several lines of evidence suggest that there are two main regulatory mechanisms in the VTA-NAc circuit: 1) dopaminergic projections from the VTA to the NAc, and 2) gamma-aminobutyric acid (GABA)ergic projections from the NAc to the VTA. These two projections regulate the neuronal function of both regions in a complementary manner (Kalivas et al., 1993; Qi et al., 2016). Additionally,

*Correspondence to:

Changjong Moon, D.V.M., M.S., Ph.D. or Heh-In Im, D.V.M., M.S., Ph.D.,
moonc@chonnam.ac.kr
or him@kist.re.kr

orcid:

0000-0003-2451-0374
(Changjong Moon)
0000-0002-4763-5009
(Heh-In Im)

doi: 10.4103/1673-5374.224374

Accepted: 2017-12-16

GABAergic neurons in the NAc receive glutamatergic projections from the hippocampus, Amy, and mPFC; these are known to modulate the rewarding and withdrawal effects induced by morphine (Russell et al., 2016).

Because MOR primarily mediates the pharmacological action of morphine, many studies have focused on the regulation of MOR when attempting to characterize the role that the NAc plays in morphine addiction (Dennis et al., 2016; Molaei et al., 2016). However, the molecular dynamics underlying the rewarding effects of morphine in the NAc remain poorly understood. Therefore, the present study utilized microarrays to evaluate the expression profiles of miRNAs in the NAc in mice that self-administered intravenous morphine. Furthermore, using various bioinformatics tools (*i.e.*, mirWalk and Database for Annotation, Visualization, and Integrated Discovery [DAVID]), the transcriptional networks between the miRNAs and their putative target mRNAs in the NAc were analyzed. In this manner, the present study was able to investigate various molecular profiles and the putative molecular networks that may be implicated in functional changes in the NAc under conditions of morphine addiction.

Materials and methods

Animals

Eighteen 7-week-old male C57BL/6 mice, weighing 23.28 ± 1.56 g, purchased from Daehan Biolink (Chungbuk, Korea), were included in this study. All mice were individually housed under a 12-hour reverse light/dark cycle in a laboratory breeding room at the Korea Institute of Science and Technology (KIST) with ad libitum access to water. For the self-administration study, we randomly divided the mice into two groups, morphine and saline infusion group (8–9 mice per group). All mice were raised under mild food restriction throughout the study (approximately 85–90% of free-feeding body weight). During the morphine self-administration periods, the mice were placed in an operant chamber enclosed within a sound-attenuating cubicle (MED-307ACT-D1; Med Associates, Inc., St. Albans, VT, USA) in a dark room. The Institutional Animal Care and Use Committee of the KIST approved all protocols used in this study (approval no. 2016-081).

Intravenous self-administration (IVSA) of procedure

Apparatus

All procedures were performed using operant chambers (29.5 cm × 32.5 cm × 23.5 cm) with two retractable levers; the left lever was used as the ‘active lever’ that allowed the mice to earn a reward. A cue light was located above each lever and programmed to turn on only when the active lever was pressed. Syringe pumps (Med Associates, Fairfax, VT, USA) were connected to an intravenous catheter placed into the external jugular vein on the back of each mouse with metal spring-covered tubes infused the morphine. The behaviors of the mice during each session were recorded, and all actions were controlled using MED-PC software (Med Associates).

Food training

Prior to IVSA of morphine, all mice were trained to press the active lever rather than the inactive lever to gain a food reward using a fixed-ratio (FR) schedule (Weeks and Collins, 1978). The schedule gradually increased from FR1 to FR5 when mice received 25 food pellets for two consecutive days, and the sessions were completed when mice received 40 food pellets. After finishing the food training at FR5, intravenous catheters were implanted into the right jugular vein of each mouse for morphine infusions. Mice were allowed to recover for 3 days, and then two food-training sessions were performed to reinstate the memory of the active lever press.

IVSA of morphine

After completion of food training, we performed IVSA of morphine. During the session of 2-hour IVSA of morphine, mice received a solution of morphine hydrochloride (Myungmoon Pharm. Co., Ltd., Seoul, South Korea) for 3 seconds at a rate of 0.01 mL/s as a reward for every active lever press; a cue light above the active lever was illuminated for 20 seconds while morphine was being infused. Because preliminary data (not shown) revealed that unit dose of 0.3 mg/kg/infusion was a stable infusion, so it was employed as a ‘training dose’ between the changing of each dose.

Morphine dose and response tests were performed using unit doses of 0.03, 1, 0.01, and 3 mg/kg/infusion. Each dose was tested for 6 days and the average number of rewards earned during the final 3 days was calculated as the reward number (morphine infusion earned). A Latin square crossover design was performed for the tests to control for any order effects during the procedure. Following dose-response tests, a morphine unit dose of 0.3 mg/kg/infusion was presented for 5 days to achieve the optimal induction of morphine addiction and sacrificed immediately after the last IVSA session. A control group of mice underwent the catheter surgery and received yoked saline infusions (13.23 ± 3.27 lever presses). The overall experimental timeline for the morphine IVSA sessions is shown in **Figure 1**.

RNA extraction from the NAc and microarray experiment procedures

Mice in the control and morphine IVSA groups were sacrificed and decapitated on the day following the final morphine IVSA session. The extracted brains were frozen and bilateral 14-gauge NAc punch dissections were obtained using a cryostat ($n = 2$ per group, CM3050S; Leica Biosystems, Nussloch GmbH, Germany). Total RNA was isolated using the RNA STAT-60 kit (Amsbio, Abingdon, UK) according to the manufacturer’s instructions. The concentration of the total RNA samples was determined by measuring optical density using the NanoDrop® ND-1000 system (Thermo Scientific, Waltham, MA, USA). miRNA expression profiling was conducted using Affymetrix GeneChip® miRNA 4.0 arrays (Affymetrix, Santa Clara, CA, USA) that contained 3,222 mature and stem-loop miRNAs. The RNA was labeled using the FlashTag™ Biotin HSR Labeling Kit (Genisphere, Hatfield, PA, USA), hybridized to the miRNA array, washed,



Figure 1 Schematic diagram of intravenous self-administration procedure.

and then scanned according to the standard Affymetrix array cassette staining protocol. Affymetrix[®] Expression Console Software version 1.2.1 (Affymetrix) was used for the last scanning step and analysis of the signals. Raw data (*.CEL files) were normalized at the transcript level using a robust multi-array average (RMA) method (Irizarry et al., 2003).

Microarray data analysis

The normalized miRNA array data were analyzed for each array. We employed fixed-fold-change (2-fold) and fixed-*P*-value ($P < 0.05$) cutoff to screen for miRNAs that exhibited significant expression patterns. Hierarchical clustering of the miRNAs was performed using the Cluster 3.0 software (<http://bonsai.hgc.jp/~mdehoo/software/cluster/software.htm>) and visualized with the MultiExperiment Viewer (<http://www.tm4.org/>).

Target prediction and pathway analysis

Responsive miRNAs were analyzed to predict putative targets using the following four databases: miRwalk 2.0 (zmf.umm.uni.heidelberg.de), miRanda (<http://www.microrna.org/>), RNA22 version 2.0 (<http://cm.jefferson.edu/rna22/Interactive/>), and Targetscan (<http://www.targetscan.org/>) in the miRwalk 2.0 platform (Dweep and Gretz, 2015). Next, the predicted targets that overlapped in at least three databases were selected for further analysis. To identify the functional pathways and reveal the miRNA/target gene regulatory network, Kyoto Encyclopedia of Genes and Genomes (KEGG; <http://www.genome.ad.jp/kegg/>) pathway analysis was applied using the predicted targets (Ogata et al., 1999). The list of target genes was used as the input for the Database for Annotation, Visualization, and Integrated Discovery (DAVID) Bioinformatics Resources 6.7 (<https://david.ncifcrf.gov/>) and the *Mus musculus* background was selected to cluster the KEGG pathways (Huang da et al., 2009).

CyTargetLinker

To show the network of miRNA and putative mRNA targets, we utilized CyTargetLinker (<http://projects.bigcat.unimass.nl/cytargetlinker/>), which is a plug-in for the Cytoscape software (<http://www.cytoscape.org/>). Representative images of the miRNA/mRNA networks were derived from the regulatory interaction networks (RegINs) provided by the MicroCosm (<http://www.ebi.ac.uk/enright-srv/microcosm/htdocs/targets/v5/>), mirTarBase (<http://mirtarbase.mbc.nctu.edu.tw/>), and TargetScan (<http://www.targetscan.org/>) databases.

Statistical analysis

All data were reported as the mean \pm SEM and analyzed with one-way analysis of variance tests using Prism 6.01 software (Graphpad Software Inc, CA, USA). Fisher's Least Significant Difference post hoc tests for multiple comparisons were performed, and *P* values < 0.05 were considered to indicate statistical significance.

Results

Mice receiving IVSA of morphine exhibited general drug-seeking behaviors

Prior to morphine infusion sessions, all mice were trained to press the active lever rather than the inactive lever to obtain food pellets as a reward in a 5-day food-training protocol conducted in the operant IVSA chamber (Figure 2A and Additional Figure 1). Following catheter implantation surgery, mice received two additional food-training sessions (Figure 2A and Additional Figure 1) before the reward was changed from food pellets to morphine infusion (0.03 mg/kg/infusion). During the first three morphine sessions, mice earned 26.33 ± 1.39 rewards on average but their mean response level was adjusted to 17.58 ± 0.84 rewards over the following six consecutive 2-hour sessions (Figure 2B, Additional Figure 1). The lever responses of the mice were also evaluated across different unit doses of morphine (0.03, 1, 0.01, and 3 mg/kg/infusion; Figure 2C–F). For all mice receiving IVSA of morphine, a dose-dependent relationship (0.01, 0.03, 0.3, 1, and 3 mg/kg/infusion) of the average infusions per lever press of the last three sessions revealed an inverted U-shaped curve (Figure 3A, B).

The number of morphine infusions ($F(4, 10) = 114.6, P < 0.001$; Figure 3A) and lever presses ($F(4, 10) = 62.10, P < 0.001$; Figure 3B) were significantly altered during the morphine self-administration session. Additionally, there were continuous increases in morphine intake across sessions for all unit doses of morphine infusion, and the volume of intake for each dose was significantly changed during morphine self-administration session ($F(4, 10) = 156.0, P < 0.001$; Figure 3C).

miRNA profiling in the NAc revealed differential expression in mice receiving IVSA of morphine

There were different patterns of miRNA expression in the NAc regions of the morphine IVSA and control mice (Figure 4). Of the 3,163 analyzed miRNAs in the NAc, there were significant alterations in 62 miRNAs after IVSA of morphine: 33 miRNAs were upregulated by more than 2-fold and 29 were downregulated by more than half (Figure 4 and Table 1).

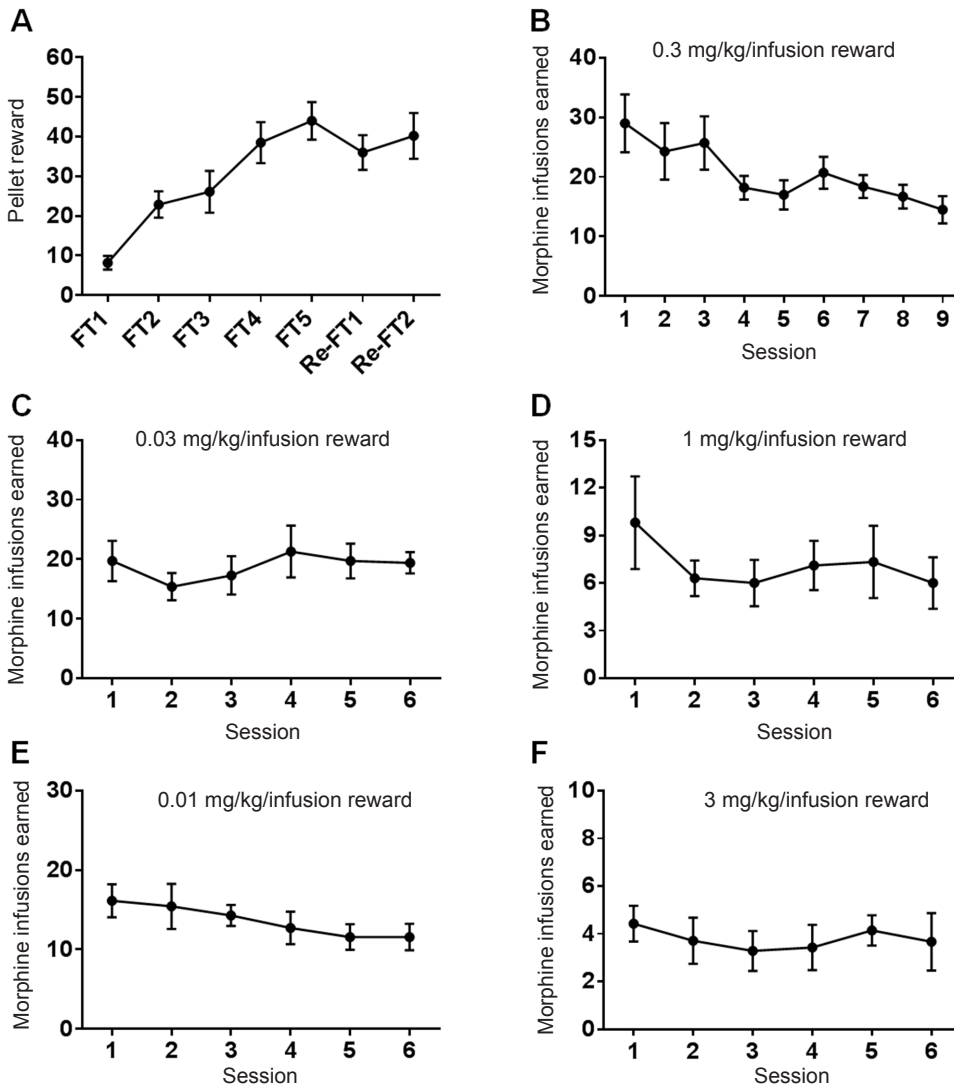


Figure 2 Mice that intravenously self-administered morphine exhibited general drug-seeking behavior. Either food pellets or intravenous morphine infusions was earned as rewards during the consecutive self-administration sessions. (A) Over five consecutive food-training sessions, the number of active lever presses to acquire food pellets gradually increased during the 1-hour sessions. Additionally, the mice underwent two additional food-training sessions following the catheter implantation surgery to reinstate their memory of the procedure. After food training, we conducted 6–9 consecutive self-administration sessions. (B) Number of morphine infusions earned and lever presses performed to receive a morphine infusion (0.3 mg/kg/infusion) during consecutive self-administration sessions. (C) Number of morphine infusions earned and lever presses performed to receive a morphine infusion (0.03 mg/kg/infusion) during consecutive self-administration sessions. (D) Number of morphine infusions earned and lever presses performed to receive a morphine infusion (1 mg/kg/infusion) during consecutive self-administration sessions. (E) Number of morphine infusions earned and lever presses performed to receive a morphine infusion (0.1 mg/kg/infusion) during consecutive self-administration sessions. (F) Number of morphine infusions earned and lever presses performed to receive a morphine infusion (3 mg/kg/infusion) during consecutive self-administration sessions. All data are reported as the mean \pm SE ($n = 8-9$ mice per dose of morphine). FT: Food training; Re-FT: re-food training.

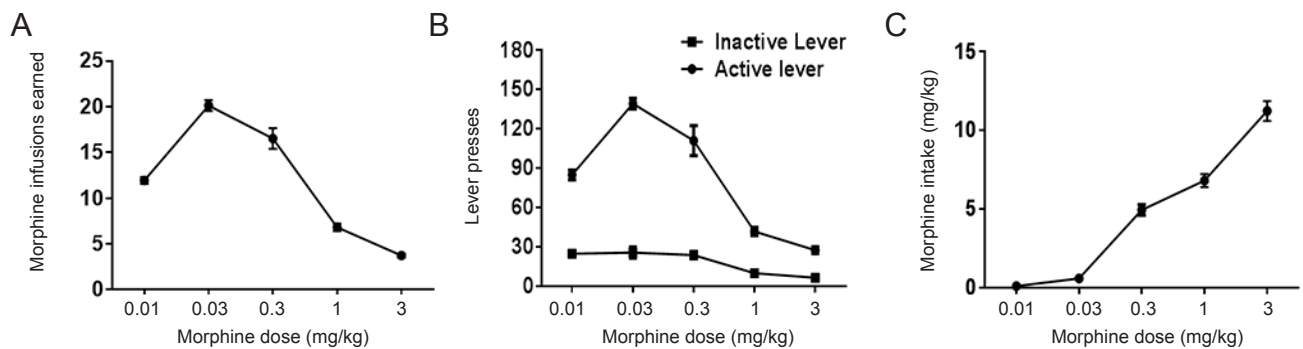


Figure 3 A typical inverted U-shaped curve in the dose-response test was generated from mice that intravenously self-administered morphine.

(A) Dose-response tests for morphine self-administration revealed relatively high numbers of infusions at unit doses of 0.03 and 0.3 mg/kg/infusions and low numbers of infusions at unit doses of 0.01, 1, and 3 mg/kg/infusions. The numbers of morphine infusions earned over the last 3 sessions were averaged for each dose. (B) The number of lever presses for morphine infusions over the last 3 sessions were averaged for each dose. (C) Total amount of morphine infused at each dose. All data are reported as mean \pm SE ($n = 8-9$ mice per dose of morphine). All data are expressed as the mean \pm standard error for each group, and analyzed with one-way analysis of variance.

Table 1 The 62 morphine responsive-miRNAs in the NAc^a

miRNA	Alignments	Sequence	Accession	Fold change	P value
Up-regulation					
mmu-miR-695	chr2:155356831-155356852 (+)	AGAUUGGGCAUAGGUGACUGAA	MIMAT0003481	20.084	0.019239
mmu-miR-32-5p	chr4:56895272-56895293 (-)	UAUUGCACAUAUACUAAGUUGCA	MIMAT0000654	13.679	0.029637
mmu-miR-202-5p	chr7:139957732-139957752 (-)	UUCCUAUGCAUAUACUUCUUU	MIMAT0004546	12.327	0.029637
mmu-miR-6899-5p	chr1:64042476-64042496 (-)	AGCAGAACGCAGCGGGCAUGA	MIMAT0027698	10.915	0.032452
mmu-miR-7231-5p	chr6:122831377-122831398 (+)	UUGGGGAACACUGGGGCAUACC	MIMAT0028430	6.641	0.017890
mmu-miR-201-5p	chrX:67988135-67988156 (-)	UACUCAGUAAGGCAUUGUUCUU	MIMAT0000234	5.153	0.047077
mmu-miR-6418-5p	chr5:137529551-137529571 (-)	UCAGGGGAAGGGAAGAGAUUC	MIMAT0025173	5.123	0.014839
mmu-miR-144-5p	chr11:78073010-78073032 (+)	GGUAUAUCAUAUACUGUAAGU	MIMAT0016988	4.754	0.047387
mmu-miR-7042-5p	chr6:113707213-113707233 (+)	UAGAGACAGCAGAAGGGCCAC	MIMAT0027988	4.687	0.034960
mmu-miR-496b	chr19:16314894-16314915 (-)	CAACAUGGCCAAUUCUUUUAUC	MIMAT0025158	4.625	0.047077
mmu-miR-6998-5p	chr2:31612426-31612447 (+)	CUGGGCAGAGGGCAAAGUGACU	MIMAT0027898	4.262	0.044504
mmu-miR-6416-3p	chr7:64249989-64250009 (-)	GCAAAGAGCAGCAAAAAGGAAG	MIMAT0025171	4.084	0.031298
mmu-miR-669d-2-3p	chr2:10471696-10471717 (+)	AUAUAUCAUACACCCAUUAC	MIMAT0014884	4.001	0.029637
mmu-miR-5619-5p	chr5:104048003-104048023 (+)	AGUCACUAUUGGCAUUUUUGU	MIMAT0022365	3.389	0.018949
mmu-miR-669d-3p	chr2:10468423-10468443 (+)	UAUAUCAUACACCCAUUAC	MIMAT0017324	3.283	0.012390
mmu-miR-6393	chr15:87795919-87795940 (-)	CUGCCACGAGGCAAGCAGUGAGU	MIMAT0025143	3.114	0.004390
mmu-miR-8117	chr5:50252823-50252843 (+)	GCUCGUGUGGAACAGAAGGGG	MIMAT0031423	3.060	0.035723
mmu-miR-3569-5p	chr7:30589380-30589400 (+)	UCGGAGGAGAGCAGACCCGUG	MIMAT0029854	2.993	0.012389
mmu-miR-669j	chr2:10477989-10478010 (+)	UGCAUAUACUCAUGCAAACA	MIMAT0005838	2.952	0.019239
mmu-miR-7670-5p	chr6:38507325-38507346 (+)	AUUCAGAUUGGGCAGAUUGGAA	MIMAT0029846	2.780	0.001239
mmu-miR-155-3p	chr16:84714182-84714202 (+)	CUCUACCUUUUAGCAUUAAC	MIMAT0016993	2.742	0.027963
mmu-miR-7578	chr2:27450549-27450572 (-)	CAUGGCUCUGUCUUCUGCCUCAGA	MIMAT0029578	2.606	0.011640
mmu-miR-8113	chr6:125234756-125234777 (-)	CAGGAGAGUCAGGGCAAGUAG	MIMAT0031419	2.551	0.027615
mmu-miR-7217-3p	chr17:27355778-27355799 (+)	UGAGAACCACAGAAGAAAGA	MIMAT0028403	2.396	0.030494
mmu-miR-669m-3p	chr2:10512847-10512868 (+)	AUAUAUCAUCCACAAACAUAU	MIMAT0009419	2.305	0.047077
mmu-miR-327	chr14:44947483-44947501 (-)	ACUUGAGGGGCAUGAGGAU	MIMAT0004867	2.169	0.019235
mmu-miR-546	chr10:126998471-126998486 (+)	AUGGUGGCACGGAGUC	MIMAT0003166	2.133	0.012825
mmu-miR-7043-5p	chr6:116646020-116646042 (-)	UGUGAAAGCAGAGAGGCAUUUU	MIMAT0027990	2.101	0.025224
mmu-miR-7118-5p	chr15:89162882-89162903 (-)	UGGGGAAGGCGGGAGAGGGAAC	MIMAT0028133	2.088	0.011466
mmu-miR-6990-3p	chr19:6914196-6914216 (-)	AGCCUUCUUCUUCUCCGCGAC	MIMAT0027883	2.071	0.021966
mmu-miR-7038-3p	chr5:140427388-140427409 (+)	CACUGCUCCUUCUUCUUCACAG	MIMAT0027981	2.048	0.036724
mmu-miR-7007-5p	chr3:20222332-20222354 (-)	UCAGAAGAGGCGAGUGGAGGAGAU	MIMAT0027918	2.041	0.040566
mmu-miR-451a	chr11:78073186-78073207 (+)	AAACCCUUAACCAUACUGAGUU	MIMAT0001632	2.008	0.026957
Down-regulation					
mmu-miR-3102-3p-2-3p	chr7:100882330-100882350 (-)	CUCUACUCCUGCCCCAGCCA	MIMAT0014935	0.482	0.031329
mmu-miR-1298-5p	chrX:147064918-147064939 (+)	UUCAUUCGGCUGUCCAGAUGUA	MIMAT0014809	0.476	0.044005
mmu-miR-3068-5p	chr12:87437724-87437747 (-)	UUGGAGUUAUGCAAAGUUCUAACC	MIMAT0014842	0.474	0.017237
mmu-miR-181a-1-3p	chr1:137966508-137966529 (+)	ACCAUCGACCCUUGAUUGUACC	MIMAT0000660	0.461	0.025901
mmu-miR-598-5p	chr14:63727199-63727221 (+)	GCGGUGAUGCCGAGUGGCGGAGC	MIMAT0017283	0.459	0.036826
mmu-miR-20b-5p	chrX:52742159-52742181 (-)	CAAAGUUCUCAUAGUGCAGUAG	MIMAT0003187	0.454	0.039668
mmu-miR-344g-5p	chr7:61982335-61982355 (-)	AGUCAGGCUCUUGGCAGGAGU	MIMAT0014929	0.452	0.011809
mmu-miR-668-5p	chr12:109734733-109734756 (+)	GUAAGUGUGCCUCGGGUGAGCAUG	MIMAT0017237	0.447	0.002704
mmu-miR-5122	chr4:133369784-133369803 (+)	CCGCGGGACCCGGGGCUGUG	MIMAT0020630	0.447	0.014469
mmu-miR-410-5p	chr12:109743729-109743749 (+)	AGGUUGUCUGUGAUGAGUUCG	MIMAT0017172	0.444	0.027598
mmu-miR-872-5p	chr4:94665167-94665187 (+)	AAGGUUAUCUUGUUAUCAGG	MIMAT0004934	0.444	0.032237
mmu-miR-1946b	chr9:21613452-21613477 (-)	GCCGGGCAGUGGCGACAUGCUUUU	MIMAT0009443	0.429	0.019378
mmu-miR-669a-5p	chr2:10474460-10474483 (+)	AGUUGUGUGGCAUGUUCUAGUCU	MIMAT0003477	0.426	0.037805
mmu-miR-669p-5p	chr2:10489130-10489153 (+)	AGUUGUGUGGCAUGUUCUAGUCU	MIMAT0014889	0.426	0.037805
mmu-miR-28a-3p	chr16:24827908-24827929 (+)	CACUAGAUUGUGAGCUGCGGA	MIMAT0004661	0.405	0.015774
mmu-miR-222-5p	chrX:19146940-19146960 (-)	UCAGUAGCCAGUUGAUAUCCU	MIMAT0017061	0.386	0.031457
mmu-miR-322-3p	chrX:53054269-53054289 (-)	AAACAUGAAGCGCUGCAACAC	MIMAT0000549	0.383	0.014835
mmu-miR-1896	chr13:21445209-21445230 (+)	CUCUCUGAUGGUGGUGAGGAG	MIMAT0007873	0.381	0.038912
mmu-miR-199a-3p	chr1:162217883-162217904 (+)	ACAGUAGUCGCAUAUUGGUAU	MIMAT0000230	0.374	0.013896
mmu-miR-199b-3p	chr2:32318524-32318545 (+)	ACAGUAGUCGCAUAUUGGUAU	MIMAT0004667	0.374	0.013896
mmu-miR-24-1-5p	chr13:63301213-63301235 (+)	GUGCCUACUGAGCUGAUUACAGU	MIMAT0000218	0.371	0.005833
mmu-miR-3110-3p	chrX:38210488-38210509 (+)	GCACUCCAUCCGAGGCAGACAC	MIMAT0014952	0.366	0.044754
mmu-miR-344d-3-5p	chr7:61726296-61726318 (-)	AGUCAGGCUAUGGUUAUACUCC	MIMAT0014807	0.362	0.047738
mmu-miR-28c	chr15:53614216-53614235 (-)	AGGAGCUCACAGUCUAUUGA	MIMAT0019339	0.354	0.022807
mmu-miR-135a-1-3p	chr9:106154179-106154200 (+)	UAUAGGGAUUGGAGCCGUGGCG	MIMAT0004531	0.347	0.048815
mmu-miR-3069-3p	chr12:105031078-105031099 (-)	UUGGACACUAAGUACUGCCACA	MIMAT0014845	0.344	0.028719
mmu-miR-344h-3p	chr7:61739350-61739371 (-)	GGUAUAACCAAGCCCGACUGU	MIMAT0022384	0.326	0.005525
mmu-miR-1982-3p	chr10:80828848-80828870 (+)	UCUCACCCUAUGUUCUCCACAG	MIMAT0009460	0.309	0.023683
mmu-miR-1981-3p	chr1:184822409-184822429 (-)	CAUCUAACCCUGCCUUUGAC	MIMAT0017351	0.201	0.018318

^aSixty-two miRNAs selected from the microarray data are presented; 33 upregulated and 29 downregulated miRNA profiles were divided and the genomic locus of the chromosome and the sequence of the miRNAs are listed. Additionally, the accessions and fold changes for each miRNA are shown.

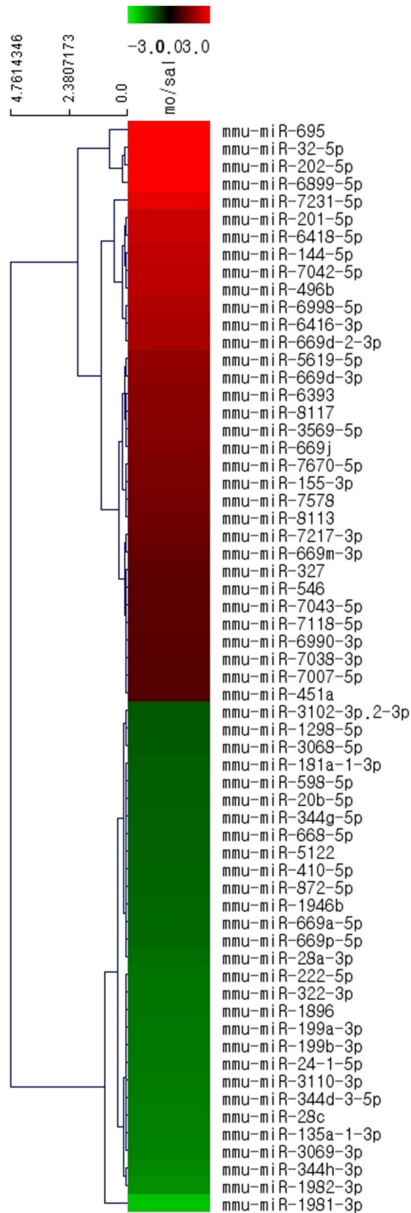


Figure 4 Accumbal miRNAs clustered after intravenous self-administration of morphine and saline. A heat map was created using significantly altered miRNAs according to the microarray data ($n = 2$); miRNA expression in the nucleus accumbens of the intravenous morphine self-administration and age-matched drug-naïve control groups were compared. The red color indicates an increased expression level and the green color indicates a decreased expression level.

An integrated analysis of the miRNA putative target network using CyTargetLinker revealed interactions in 62 NAc miRNAs following morphine self-administration

To assess the relationships between the miRNAs and their putative mRNAs, 62 responsive miRNAs were analyzed using CyTargetLinker; the representative networks of the miRNAs and their putative targets were derived from RegINs and the interactions of each network were analyzed within the whole network. Among the upregulated miRNAs, mmu-miR-32-5p was associated with mmu-miR-451a to regulate their common target, *Nsmal*, and interacted with mmu-

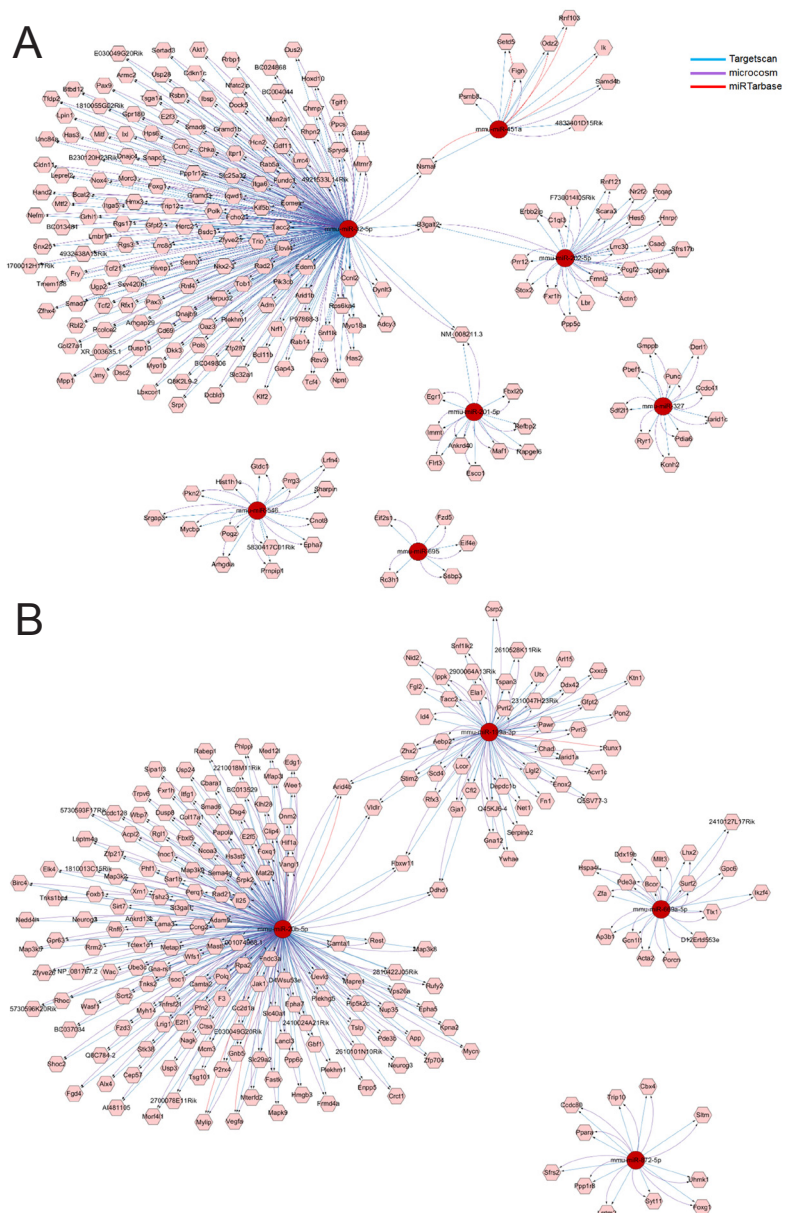


Figure 5 Representative miRNA/target interaction networks in the NAc created using CyTargetLinker following morphine self-administration.

Based on the miRNA array data, we divided the responsive miRNAs into increased miRNAs and decreased miRNAs groups. After that, we used CyTargetLinker to show the interaction between responsive miRNAs and predicted target gene interaction after morphine self-administration. (A) Increased miRNAs-mRNA and (B) decreased miRNAs-mRNA showed diverse patterns of networks.

miR-202-5p to regulate *B3galt2*, while mmu-miR-32-5p and mmu-miR-201-5p were associated with the regulation of *NM_008211.3* (Figure 5A). Of the downregulated miRNAs, mmu-miR-20b-5p and mmu-miR-193-3p shared the following four common targets: *Arid4b*, *Vldlr*, *Fbxw11*, and *Ddhd1* (Figure 5B).

miRNAs altered by morphine self-administration had putative targets related to various functions of the NAc

In the present study, 62 responsive miRNAs were analyzed for putative target detection using miRwalk 2.0 web, mi-

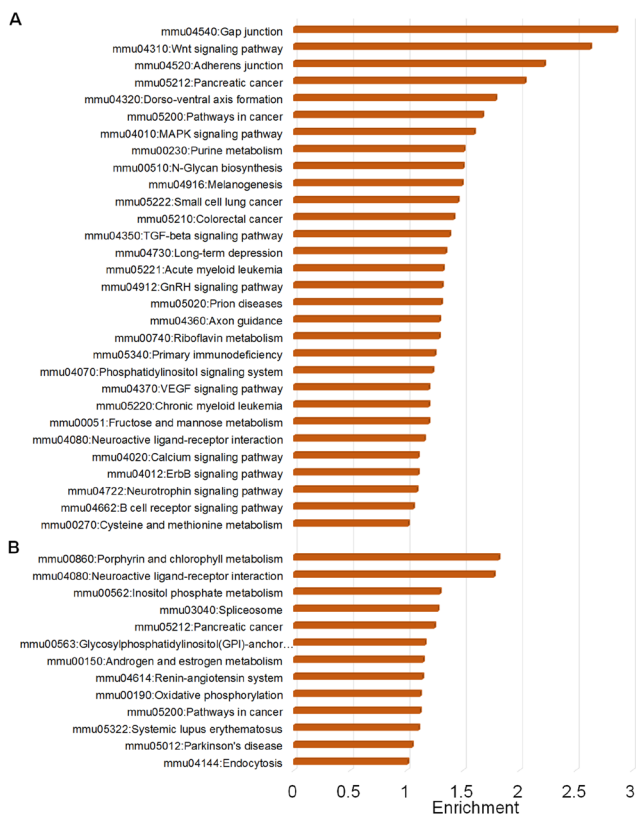


Figure 6 Classification of predicted target genes by morphine-responsive miRNAs according to the KEGG pathway analysis. A total of 62 altered miRNAs were analyzed based on the target prediction algorithms of the bioinformatics database. KEGG pathways targeted by (A) upregulated and (B) downregulated miRNAs in the NAc. The vertical axis represents the pathway categories and the horizontal axis represents pathway enrichment calculated as $-\log$ [modified Fisher's exact P -value].

Randa, RNA22 version 2.0, and TargetScan. Of the putative targets derived using these four algorithms, 7,752 predicted mRNAs were potentially regulated by 62 miRNAs. A functional categorization of the target genes was performed using the DAVID functional annotation tool (<https://david.ncifcrf.gov>) prior to analysis using the KEGG Pathways (Figure 6). A total of 43 different pathways corresponded to the altered miRNAs and several pathways, including Wnt signaling, mitogen-activated protein kinase (MAPK) signaling, transforming growth factor- β (TGF- β) signaling, long-term depression (LTD), calcium (Ca^{2+}) signaling, and endocytosis pathways (Figure 6 and Additional Figures 2–7), are thought to be involved in neuronal function.

Discussion

The present study is the first to examine the distinct expression patterns and functional roles of miRNAs in the NAc using a mouse model of morphine addiction. Two different expression patterns (upregulation and downregulation) of miRNA in mice receiving IVSA of morphine were compared to those in drug-naïve mice to determine the functional categorization of the miRNA targets associated with morphine

addiction. Additionally, a bioinformatics analysis of the dynamic interactions within the miRNA target network was performed to characterize the roles of potential target mRNAs in the clinical symptoms of morphine addiction.

Current research indicates that the NAc plays a central role in the regulation of behavioral functions associated with depression, anxiety, and addiction due to its involvement in the brain reward circuit (Di Chiara and Imperato, 1988; Polter and Kauer, 2014). Approximately 95% of cells within the NAc are GABAergic neurons that possess dopamine D1- and D2-like receptors (Koo et al., 2014). NAc function is influenced by dopaminergic projections from the VTA (Fields and Margolis, 2015) and numerous studies have indicated that the high level of MOR distribution in the NAc might be related to the behavioral properties of opioid addiction, including reward and withdrawal symptoms (Dennis et al., 2016; Han et al., 2010). These behavioral consequences are reported to result from neuronal dysfunction induced by chronic exposure to opioids (Cunha-Oliveira et al., 2008; Ferrini et al., 2013). Therefore, identifying changes in NAc signaling pathways may be essential for a complete understanding of the mechanisms underlying the development of addictive behaviors.

According to the KEGG pathway analyses, 15 miRNAs and 45 of their putative targets appear to regulate the Wnt, MAPK, TGF- β , and neurotrophin signaling pathways, which are involved in diverse neuronal functions, such as neurogenesis, synaptic plasticity, and neuroinflammation (Fakira et al., 2014; Sanna et al., 2014; Zhang et al., 2016). Additionally, some of the miRNAs had multiple targets in each signaling pathway. In the Wnt signaling pathway, mmu-miR-202-5p regulated *Fbxw11* and *TBL1xr1*; mmu-669d-2-3p regulated *ROCK2*, *SMAD2*, *FZD7*, and *FZD10*; and mmu-miR-32-5p regulated *DKK2*, *MAPK8*, and *FZD10*. In the MAPK signaling pathway, mmu-669d-2-3p regulated *CHUK*, *RASA2*, *PTPRR*, *DUSP10*, and *CACNA1G*; and mmu-miR-32-5p regulated *ELK4*, *MAP2K4*, and *MAPK8*. In the TGF- β signaling pathway, mmu-miR-669d-2-3p and mmu-miR-669-3p shared several target genes, including *ROCK2*, *NODAL*, and *SMAD2*, and mmu-miR-6416-3p regulated *SMAD1* and *LEFTY1*. In the neurotrophin signaling pathway, mmu-miR-496b regulated *IRS2* and *MAP2K1* and mmu-miR-32-5p regulated *PIK3CB* and *MAPK8*.

Previous studies have suggested that there is a relationship between acute/chronic morphine treatment and synaptic plasticity in terms of Ca^{2+} -dependent signaling in glutamatergic transmission (Chartoff and Connery, 2014) and that the NAc exhibits different types of intracellular signaling during the acute and chronic phases of morphine exposure (Nestler, 2004; Chartoff and Connery, 2014). During the acute phase of exposure, morphine inhibits presynaptic voltage-gated Ca^{2+} currents and upregulates protein kinase C (PKC)-dependent signaling (Martin et al., 1997), whereas morphine increases α -amino-3-hydroxy-5-methyl-4-isoxazolepropionic acid (AMPA) and N-methyl-D-aspartate (NMDA)-mediated synaptic transmission during the

chronic phase of exposure (Martin et al., 1997; Xu et al., 2012; Chartoff and Connery, 2014). In the present study, the KEGG analysis of putative targets for the altered miRNAs revealed that the regulatory pathway for Ca²⁺-dependent signaling was involved in the mouse model of morphine addiction.

It is known that individuals addicted to psychostimulants suffer from a variety of emotional states, such as depression or anxiety, which are caused by disruptions in LTD and long-term potentiation (LTP) (Nestler, 2001; Kasanetz et al., 2010). The KEGG pathway analysis in the present study identified a significant upregulation of mmu-miR-202-5p, which potentially regulates the LTD-associated genes PLC- β and KRAs. This is consistent with previous findings showing that morphine exposure modulates LTD in the NAc via mGLUR2/3 abolition during the withdrawal phase (Robbe et al., 2002) and that GABAergic synapses on VTA dopaminergic neurons are capable of inducing LTD while morphine stimulation significantly reduces LTD in the VTA (Dacher and Nugent, 2011).

Morphine is known for its rapid induction of tolerance, which limits its clinical use for anti-nociception (Gonzalez et al., 1997). Recent studies have suggested that the failure of morphine to promote MOR endocytosis can cause MOR desensitization, which, in turn, induces morphine tolerance and dependence (Kim et al., 2008; Berger and Whistler, 2010). The KEGG analysis of the putative targets for responsive miRNAs in the NAc after morphine self-administration in the present study identified 25 mRNAs that regulated endocytosis: *FGFR2*, *EGFR*, *RET*, *CHMP5*, *TSG101*, *ASAP2*, *ARF6*, *EEA1*, *LDLRAP1*, *CHMP2B*, *ACVR1B*, *RAB11FIP5*, *DAB2*, *SH3GLB1*, *LOC547349*, *RAB22A*, *RAB11B*, *GRK6*, *RAB11A*, *HGS*, *PARD6G*, *EHD1*, *IQSEC1*, *EHD3*, and *RNF41*.

To the best of our knowledge, this is the first study to perform a bioinformatics analysis of the networks between miRNAs and their putative targets in the NAc of mice intravenously self-administered morphine. Using this paradigm, a set of accumbal miRNAs that were altered by chronic morphine exposure were defined, and Wnt signaling, MAPK signaling, TGF- β signaling, LTD, calcium signaling, and endocytosis likely play important roles in morphine addiction. However, it is important to note that the networks among these miRNAs and their putative target genes were investigated using only a bioinformatics analysis; therefore, *in vitro* and *in vivo* experiments are needed to validate the links in these miRNA/mRNA networks and the functional effects of their changes on morphine addiction. Furthermore, it is likely necessary to determine the miRNA expression levels in specific brain regions and/or serum of humans/primates with morphine addiction.

Author contributions: JK, HII, and CM designed the study, performed experiments, collected experimental data, and wrote the paper. All authors approved the final version of this paper.

Conflicts of interest: None declared.

Financial support: This research was funded by the National Research

Council of Science & Technology (NST) grant by the Korean government (MSIP) (No. CRC-15-04-KIST) and the National Research Foundation of Korea under the grant (No. NRF-2017R1A2B200399; Mid-career Researcher Program). The funding bodies played no role in the study design, in the collection, analysis and interpretation of data, in the writing of the manuscript, and in the decision to submit the manuscript for publication.

Research ethics: All experiments were approved by the Institutional Animal Care and Use Committee of the KIST (approval No. 2016-081).

Data sharing statement: Datasets analyzed during the current study are available from the corresponding author on reasonable request.

Plagiarism check: Checked twice by iThenticate.

Peer review: Externally peer reviewed.

Open access statement: This is an open access article distributed under the terms of the Creative Commons Attribution-NonCommercial-ShareAlike 3.0 License, which allows others to remix, tweak, and build upon the work non-commercially, as long as the author is credited and the new creations are licensed under identical terms.

Open peer reviewers: Puneet Bagga, University of Pennsylvania Perelman School of Medicine, USA; Murat Sahin, University of Amasya, Faculty of Medicine, Turkey.

Additional file:

Additional Figure 1: Lever presses in the operant chamber during morphine intravenous self-administration.

Additional Figure 2: KEGG pathway analysis of the Wnt signaling pathway.

Additional Figure 3: KEGG pathway analysis of the MAPK signaling pathway.

Additional Figure 4: KEGG pathway analysis of the TGF- β signaling pathway.

Additional Figure 5: KEGG pathway analysis of the LTD pathway.

Additional Figure 6: KEGG pathway analysis of the Ca²⁺ signaling pathway.

Additional Figure 7: KEGG pathway analysis of the endocytosis pathway.

References

- Beier KT, Steinberg EE, DeLoach KE, Xie S, Miyamichi K, Schwarz L, Gao XJ, Kremer EJ, Malenka RC, Luo L (2015) Circuit architecture of VTA dopamine neurons revealed by systematic input-output mapping. *Cell* 162:622-634.
- Berger AC, Whistler JL (2010) How to design an opioid drug that causes reduced tolerance and dependence. *Ann Neurol* 67:559-569.
- Chartoff EH, Connery HS (2014) It's MORE exciting than mu: cross-talk between mu opioid receptors and glutamatergic transmission in the mesolimbic dopamine system. *Front Pharmacol* 5:116.
- Cunha-Oliveira T, Rego AC, Oliveira CR (2008) Cellular and molecular mechanisms involved in the neurotoxicity of opioid and psychostimulant drugs. *Brain Res Rev* 58:192-208.
- Dacher M, Nugent FS (2011) Morphine-induced modulation of LTD at GABAergic synapses in the ventral tegmental area. *Neuropharmacology* 61:1166-1171.
- Dalal S, Hui D, Nguyen L, Chacko R, Scott C, Roberts L, Bruera E (2012) Achievement of personalized pain goal in cancer patients referred to a supportive care clinic at a comprehensive cancer center. *Cancer* 118:3869-3877.
- Dennis TS, Beck KD, Cominski TP, Bobzean SA, Kuzhikandathil EV, Servatius RJ, Perrotti LI (2016) Exposure to morphine-associated cues increases mu opioid receptor mRNA expression in the nucleus accumbens of Wistar Kyoto rats. *Behav Brain Res* 313:208-213.
- Di Chiara G, Imperato A (1988) Drugs abused by humans preferentially increase synaptic dopamine concentrations in the mesolimbic system of freely moving rats. *Proc Natl Acad Sci USA* 85:5274-5278.
- Dweep H, Gretz N (2015) miRWalk2.0: a comprehensive atlas of microRNA-target interactions. *Nat Methods* 12:697.
- Fakira AK, Portugal GS, Carusillo B, Melyan Z, Moron JA (2014) Increased small conductance calcium-activated potassium type 2 channel-mediated negative feedback on N-methyl-D-aspartate receptors impairs synaptic plasticity following context-dependent sensitization to morphine. *Biol Psychiatry* 75:105-114.

- Ferrini F, Trang T, Mattioli TA, Laffray S, Del'Guidice T, Lorenzo LE, Castonguay A, Doyon N, Zhang W, Godin AG, Mohr D, Beggs S, Vandal K, Beaulieu JM, Cahill CM, Salter MW, De Koninck Y (2013) Morphine hyperalgesia gated through microglia-mediated disruption of neuronal Cl(-) homeostasis. *Nat Neurosci* 16:183-192.
- Fields HL, Margolis EB (2015) Understanding opioid reward. *Trends Neurosci* 38:217-225.
- Fitting S, Stevens DL, Khan FA, Scoggins KL, Enga RM, Beardsley PM, Knapp PE, Dewey WL, Hauser KF (2016) Morphine tolerance and physical dependence are altered in conditional HIV-1 Tat transgenic mice. *J Pharmacol Exp Ther* 356:96-105.
- Gonzalez P, Cabello P, Germany A, Norris B, Contreras E (1997) Decrease of tolerance to, and physical dependence on morphine by, glutamate receptor antagonists. *Eur J Pharmacol* 332:257-262.
- Han MH, Renthal W, Ring RH, Rahman Z, Psifogeorgou K, Howland D, Birnbaum S, Young K, Neve R, Nestler EJ, Zachariou V (2010) Brain region specific actions of regulator of G protein signaling 4 oppose morphine reward and dependence but promote analgesia. *Biol Psychiatry* 67:761-769.
- Hollander JA, Im H-I, Amelio AL, Kocerha J, Bali P, Lu Q, Willoughby D, Wahlestedt C, Conkright MD, Kenny PJ (2010) Striatal microRNA controls cocaine intake through CREB signalling. *Nature* 466:197-202.
- Huang da W, Sherman BT, Lempicki RA (2009) Systematic and integrative analysis of large gene lists using DAVID bioinformatics resources. *Nat Protoc* 4:44-57.
- Im HI, Hollander JA, Bali P, Kenny PJ (2010) MeCP2 controls BDNF expression and cocaine intake through homeostatic interactions with microRNA-212. *Nat Neurosci* 13:1120-1127.
- Im HI, Kenny PJ (2012) MicroRNAs in neuronal function and dysfunction. *Trends Neurosci* 35:325-334.
- Imperio CG, McFalls AJ, Colechio EM, Masser DR, Vrana KE, Grigson PS, Freeman WM (2016) Assessment of individual differences in the rat nucleus accumbens transcriptome following taste-heroin extended access. *Brain Res Bull* 123:71-80.
- Irizarry RA, Hobbs B, Collin F, Beazer-Barclay YD, Antonellis KJ, Scherf U, Speed TP (2003) Exploration, normalization, and summaries of high density oligonucleotide array probe level data. *Bio-statistics* 4:249-264.
- Jonas S, Izaurralde E (2015) Towards a molecular understanding of microRNA-mediated gene silencing. *Nat Rev Genet* 16:421-433.
- Kalivas PW, Churchill L, Klitenick MA (1993) GABA and enkephalin projection from the nucleus accumbens and ventral pallidum to the ventral tegmental area. *Neuroscience* 57:1047-1060.
- Kasanetz F, Deroche-Gamonet V, Berson N, Balado E, Lafourcade M, Manzoni O, Piazza PV (2010) Transition to addiction is associated with a persistent impairment in synaptic plasticity. *Science* 328:1709-1712.
- Kim J, Ham S, Hong H, Moon C, Im HI (2016) Brain reward circuits in morphine addiction. *Mol Cells* 39:645-653.
- Kim JA, Bartlett S, He L, Nielsen CK, Chang AM, Kharazia V, Waldhoer M, Ou CJ, Taylor S, Ferwerda M, Cado D, Whistler JL (2008) Morphine-induced receptor endocytosis in a novel knockin mouse reduces tolerance and dependence. *Curr Biol* 18:129-135.
- Koo JW, Lobo MK, Chaudhury D, Labonte B, Friedman A, Heller E, Pena CJ, Han MH, Nestler EJ (2014) Loss of BDNF signaling in D1R-expressing NAc neurons enhances morphine reward by reducing GABA inhibition. *Neuropsychopharmacology* 39:2646-2653.
- Martin G, Nie Z, Siggins GR (1997) mu-Opioid receptors modulate NMDA receptor-mediated responses in nucleus accumbens neurons. *J Neurosci* 17:11-22.
- Molaei M, Fatahi Z, Zaringhalam J, Haghparast A (2016) CB1 cannabinoid agonist (WIN55,212-2) within the basolateral amygdala induced sensitization to morphine and increased the level of mu-opioid receptor and c-fos in the nucleus accumbens. *J Mol Neurosci* 58:446-455.
- Nestler EJ (2001) Molecular basis of long-term plasticity underlying addiction. *Nat Rev Neurosci* 2:119-128.
- Nestler EJ (2004) Historical review: molecular and cellular mechanisms of opiate and cocaine addiction. *Trends Pharm Sci* 25:210-218.
- Ogata H, Goto S, Sato K, Fujibuchi W, Bono H, Kanehisa M (1999) KEGG: kyoto encyclopedia of genes and genomes. *Nucleic Acids Res* 27:29-34.
- Parker KE, Johns HW, Floros TG, Will MJ (2014) Central amygdala opioid transmission is necessary for increased high-fat intake following 24-h food deprivation, but not following intra-accumbens opioid administration. *Behav Brain Res* 260:131-138.
- Polter AM, Kauer JA (2014) Stress and VTA synapses: implications for addiction and depression. *Eur J Neurosci* 39:1179-1188.
- Qi J, Zhang S, Wang HL, Barker DJ, Miranda-Barrientos J, Morales M (2016) VTA glutamatergic inputs to nucleus accumbens drive aversion by acting on GABAergic interneurons. *Nat Neurosci* 19:725-733.
- Raphael JH, Duarte RV, Southall JL, Nightingale P, Kitas GD (2013) Randomised, double-blind controlled trial by dose reduction of implanted intrathecal morphine delivery in chronic non-cancer pain. *BMJ Open* 3.
- Robbe D, Bockaert J, Manzoni OJ (2002) Metabotropic glutamate receptor 2/3-dependent long-term depression in the nucleus accumbens is blocked in morphine withdrawn mice. *Eur J Neurosci* 16:2231-2235.
- Russell SE, Puttick DJ, Sawyer AM, Potter DN, Mague S, Carlezon WA, Jr., Chartoff EH (2016) Nucleus accumbens AMPA receptors are necessary for morphine-withdrawal-induced negative-affective states in rats. *J Neurosci* 36:5748-5762.
- Russo SJ, Dietz DM, Dumitriu D, Morrison JH, Malenka RC, Nestler EJ (2010) The addicted synapse: mechanisms of synaptic and structural plasticity in nucleus accumbens. *Trends Neurosci* 33:267-276.
- Russo SJ, Nestler EJ (2013) The brain reward circuitry in mood disorders. *Nat Rev Neurosci* 14:609-625.
- Sanna MD, Ghelardini C, Galeotti N (2014) Regionally selective activation of ERK and JNK in morphine paradoxical hyperalgesia: a step toward improving opioid pain therapy. *Neuropharmacology* 86:67-77.
- Tan SE (2008) Roles of hippocampal NMDA receptors and nucleus accumbens D1 receptors in the amphetamine-produced conditioned place preference in rats. *Brain Res Bull* 77:412-419.
- Weeks JR, Collins RJ (1978) Self-administration of morphine in the rat: relative influence of fixed ratio and time-out. *Pharmacol Biochem Behav* 9:703-704.
- Xu Y, Lv XF, Cui CL, Ge FF, Li YJ, Zhang HL (2012) Essential role of NR2B-containing NMDA receptor-ERK pathway in nucleus accumbens shell in morphine-associated contextual memory. *Brain Res Bull* 89:22-30.
- Zhang Y, Xu C, Zheng H, Loh HH, Law PY (2016) Morphine modulates adult neurogenesis and contextual memory by impeding the maturation of neural progenitors. *PLoS One* 11:e0153628.

(Copyedited by Li CH, Song LP, Zhao M)